

Article

New Insights into Aromaticity through Novel Delta Polynomials and Delta Aromatic Indices

Krishnan Balasubramanian

School of Molecular Sciences, Arizona State University, Tempe, AZ 85287-1604, USA; kbalu@asu.edu

Abstract: We have developed novel polynomials called delta polynomials, which are, in turn, derived from the characteristic and matching polynomials of graphs associated with polycyclic aromatic compounds. Natural logarithmic aromatic indices are derived from these delta polynomials, which are shown to provide new insights into the aromaticity of polycyclic aromatic compounds, including the highly symmetric C_{60} buckminsterfullerene, several other fullerenes, graphene, kekulene series and other cycloarenes, such as polycyclic circumcoronaphenes and coronoids. The newly developed aromatic index yields a value of 6.77 for graphene, 6.516865 for buckminsterfullerene $C_{60}(I_h)$, 5.914023 for kekulene (D_{6h} symmetry), 6.064420 for coronene (D_{6h}), 6.137828 for circumcoronene (D_{6h}), 6.069668 for dicronylene and so forth. Hence, the novel scaled logarithmic aromatic delta indices developed here appear to provide good quantitative measures of aromaticity, especially when they are used in conjunction with other aromatic indicators.

Keywords: aromaticity; delta polynomials; delta aromatic indices; characteristic; matching polynomials; aromaticity measures; topological aromatic measures

1. Introduction

The concept of aromaticity has intrigued both experimental [1–12] and theoretical chemists [13–69] resulting in a plethora of publications on the topic over the decades. The landscape of aromatic compounds has dramatically metamorphosed with the advent of molecules such as the highly symmetric buckminsterfullerene [1]; various fullerenes [2]; and circumcised coronoidal polycyclic aromatics, such as kekulene [3–5], septulene [6], octulene [7], porous nanographenes [9–16] and so forth. Consequently, the old concepts of aromaticity that included primarily planar polycyclic compounds with $4n + 2$ π -electrons has evolved into intriguing concepts such as the 3D-aromaticity, spherical aromaticity, superaromaticity, etc., and thus encompass non-planar compounds and even compounds that do not strictly conform to the $4n + 2$ π -electron rule. Circumcised coronoidal polycyclic aromatic compounds that display extended macrocyclic conjugation such as circumkekulene, non-alternant septulene [6], nanographenes [9–16] and the truncated icosahedral C_{60} with I_h symmetry [1,2], the cynosure of fullerenes, have all contributed to the evolution of the topics of aromaticity and superaromaticity to encompass such a large array of varied compounds in striking contrast to planar polycyclics with $4n + 2$ π -electrons [1–69]. Consequently, the aromaticity concept continues to challenge our understanding owing to the enhanced thermodynamic stability of several of these polycyclic compounds that can only be explained through the generalization of these concepts to encompass the phenomenon of superaromaticity and spherical aromaticity. Yet aromaticity continues to be an elusive concept, defying our established conceptual platforms and pointing to the compelling requirement for the development of novel ideas to encompass such a varied platform of polycyclic compounds that exhibit enhanced thermodynamic or kinetic stabilities.

The advent of kekulene [3–5], a circumcised coronene with D_{6h} symmetry, demonstrates the existence of a structure with a cavity made possible by an assembly of angularly annulated benzene rings which arises from a combination of two interacting $[4n + 2]$ annulenes. The enhanced thermodynamic stability of kekulene is experimentally demonstrated



Citation: Balasubramanian, K. New Insights into Aromaticity through Novel Delta Polynomials and Delta Aromatic Indices. *Symmetry* **2024**, *16*, 391. <https://doi.org/10.3390/sym16040391>

Academic Editor: György Keglevich

Received: 6 March 2024

Revised: 19 March 2024

Accepted: 20 March 2024

Published: 27 March 2024



Copyright: © 2024 by the author. Licensee MDPI, Basel, Switzerland. This article is an open access article distributed under the terms and conditions of the Creative Commons Attribution (CC BY) license (<https://creativecommons.org/licenses/by/4.0/>).

with the synthesis of this molecule and the observed proton NMR chemical shifts and magnetic properties—all of which suggest that the extended ring currents arise from individual benzene rings [3–5], as opposed to overly extended delocalizations around the entire structure. Furthermore, sister polyarene molecules with cavities such as septulene and octulene have been synthesized over the years [6,7], although septulene, with a seven-fold symmetry exhibiting the D_{7h} point group, does not conform to the traditional notion of an alternant polycyclic aromatic compound. Notwithstanding the fact that septulene [6] is not alternant and does not conform to the typical $[4n + 2]$ rule, it exhibits electronic and magnetic properties that are reminiscent of kekulene, provoking us to revisit our conventional notions of aromatic compounds.

Topological, group theoretical and graph theoretical techniques [13–70] have been developed and applied to a large number of polycyclic aromatic compounds, organic polymers, fullerenes, circumcised coronoidal structures with cavities, nanographenes and so forth with the objective of shedding light on their structures, spectra, combinatorial chemistry, properties, magnetic and electronic features, aromaticity and toxicity. One such technique that has enjoyed considerable success is the conjugated circuit theory [42–44,65], which relies on the combinatorial enumeration of inherent conjugated circuits and Clar's aromatic sextets [19,28,40]. The technique has facilitated a reliable platform for understanding the relative stabilities, aromaticity and magnetic and electronic properties of polycyclic aromatics. Furthermore, such combinatorial and graph theoretical methods have provided significant new insights into intriguing phenomena such as superaromaticity, which is a form of macrocyclic aromaticity. These techniques have revealed that the macrocyclic conjugation inherent to these structures is the primary cause of their enhanced thermodynamic stability. Combinatorics and graph theory have been applied to the enumeration of conjugated circuits, isomers of polycyclic aromatics and their derivatives, spectral polynomials, matching polynomials, distance polynomials and a number of polycyclic aromatics and fullerene cages [13–76]. An intriguing feature of such applications is that some of these symmetry-based techniques involve such novel group theoretical techniques, such as Euler's totient functions, Polya's theory of enumeration, etc., to predict their polysubstituted isomers and spectra [77]. Many of these polysubstituted aromatics, macrocyclic arenes, heteropolycyclic arenes and related halocarbons have been studied owing to their significant importance as environmental pollutants, carcinogens, hepatotoxins, industrial chemicals and petroleum products. Furthermore, macrocyclic compounds find applications in the environmental remediation through the selective sequestration of metal ions, and consequently, they find important applications in the sequestration of toxic metal ions, for example, in high-level nuclear wastes. Hosoya [21] has carried out pioneering studies connecting symmetry and matchings of graphs and extensive work has been carried out by Hosoya [18–24], Aihara [13,23,25,26,29–33,35,40,49–55], Dias [34–39,53,56–58] and the author and coworkers [16,66–76] connecting such polynomials, graph theoretical concepts, resonance energies and so forth to gain insights into aromaticity.

The above survey of experimental and theoretical interest in aromaticity and polycyclic compounds clearly demonstrates significant interest in the topic and the somewhat elusive nature of aromaticity. Despite all these developments, aromaticity continues to baffle researchers in this field due to the varied complexity of compounds that belong to this class. Stimulated by several pioneering conceptual studies that we have cited herein, the present work extends several of these ideas to encompass both characteristic and matching polynomials to evolve into novel aromatic scaled delta and zeta indices together with delta polynomials. We have knitted many of these concepts into a novel fabric of aromaticity in order to apply these concepts to a vast array of polycyclics, including three-dimensional fullerenes and polycyclic structures containing cavities as well as conventional polycyclic aromatics. We demonstrate the utility of delta polynomials and the novel indices that we propose in this study for a variety of such compounds.

2. Delta Polynomials: Mathematical and Computational Methods

We start with the definition of the adjacency matrix of a graph:

$$A_{ij} = \begin{cases} 1 & \text{if vertices } i \text{ and } j \text{ are connected} \\ 0 & \text{otherwise} \end{cases}$$

An important graph-theoretical invariant, although not unique, is the characteristic polynomial of the graph, denoted by P_G . The characteristic or the spectral polynomial of a graph is given by:

$$P_G(x) = |xI - A| = C_n x^n + C_{n-1} x^{n-1} + \dots + C_1 x + C_0$$

where C_k is the k th coefficient in the characteristic polynomial, which can be interpreted combinatorically through Sachs' theorem:

$$C_k = \sum_{g \in G_i} (-1)^{c(g)} 2^{r(g)}$$

G_i is Sachs' subgraph of G containing k vertices; $c(g)$ is the disconnected components in g ; and $r(g)$ is the number of cycles in the subgraph g . The related matching polynomial or the acyclic polynomial of a graph G can be defined with $p(G, k)$, which is the number of ways to place k disjoint dimers on the graph G :

$$M_G(x) = \sum_{k=0}^{\lfloor \frac{n}{2} \rfloor} (-1)^k p(G, k) x^{n-2k}$$

where $\lfloor n/2 \rfloor$ is the greatest integer contained in $n/2$. For any graph containing an even number of vertices, the coefficients of the odd terms are zero, and consequently, they are not included in the above definition of the matching polynomials. We also note that the constant coefficient in the matching polynomial enumerates the number of Kekulé structures or full coverings with matching for any graph G . Another way to express the matching polynomial that would include zero alternating coefficients is:

$$M_G(x) = \sum_{k=0}^n (-1)^k a_k x^{n-k}$$

where a_k is zero for odd terms while it is the number of dimers for even terms. Hence, a_k is sometimes called the acyclic coefficient, while $M_G(x)$ is also referred to as the acyclic polynomial as it contains the acyclic components of Sachs' subgraphs in G . The above definition is more convenient to compare the matching polynomial and the characteristic polynomial of a graph.

The spectra of a graph G are simply the eigenvalues of the adjacency matrix or the roots of the characteristic polynomial as defined above. Likewise, the roots of the matching polynomial constitute the matching spectra of G . For several graphs, the present author [74] showed that the matching spectra are the eigenvalues of complex-edge-weighted graph derived from G by assigning complex weights so that the overall adjacency matrix is hermitian. Moreover, Hosoya and the author [78,79] have shown that the matching polynomials of a number of graphs can be obtained as the characteristic polynomials of complex-edge weighted graphs, although these techniques are restricted to a few graphs and the weighting scheme becomes more complicated for larger graphs containing multiple fused cycles. As shown by Aihara [33], an important insight can be obtained into aromaticity through the concept of topological resonance energy, which is obtained as the weighted algebraic sum of the difference between graph spectral eigenvalues and the matching spectral values. Although this is an important measure of aromaticity, it is a difficult quantity to deal with as the matching spectra of graphs containing a large number of vertices with several fused cycles as in polycyclic aromatic compounds are difficult to obtain, although the graph spectra can be more readily obtained by diagonalizing the adjacency matrix by invoking symmetry or by the standard Givens–Householder tri-diagonalization technique. Even for

graphs containing a very large number of vertices, it has been shown that the Hadamard transform technique can be employed to extract all eigenvalues of the adjacency matrix [80].

Consequently, the bottleneck of the topological resonance energy computation lies in the computation of matching spectra for highly clustered graphs containing large numbers of vertices. Although Aihara [33] suggested the use of bond resonance energy and circuit resonance energy to circumvent this difficulty, the quantitative measures of aromaticity continue to pose challenges for graphs containing multiple fused cycles with a large number of vertices.

Stimulated by the works of Hosoya [18–24] as well as Hosoya and the current author [78,79], we propose here novel polynomials which we call delta polynomials and derive natural logarithmic aromatic indices from the coefficients of delta polynomials. The delta polynomial for any graph is defined as follows:

$$\delta_G(x) = \sum_{k=0}^n |C_k - a_k| x^{n-k} = \sum_{k=0}^n \delta_k x^{n-k}$$

where C_k and a_k are the coefficients from the characteristic polynomial and matching polynomial, respectively. We note that the coefficients in the delta polynomial are always non-negative, and the first few terms of the delta polynomial tend to be zero. Moreover, for trees or acyclic polyenes, all coefficients in the delta polynomials are identically zero because the matching and characteristic polynomials become identical for trees. As seen from Sachs' theorem, the coefficients of the characteristic polynomials contain both cyclic and acyclic components while the coefficients of the matching polynomials contain purely acyclic components. Consequently, delta polynomials contain all important cyclic components of various lengths together with some dimeric components, and thus include several important measures required to provide quantitative measures of aromaticity. However, as these coefficients tend to increase in magnitude sharply for larger graphs, we define two aromatic indices based on the coefficients of delta polynomials.

$$\Delta_a = \frac{1}{n} \ln(\sum |\delta_k|),$$

$$\Delta_w = \frac{1}{n} \ln(\sum k |\delta_k|),$$

where the sum is taken over all non-zero coefficients of the delta polynomial and n is the number of vertices in the graph. The second aromatic index is considered a weighted index, as it includes the lengths of various components that are purely non-acyclic. Note that for comparison, Hosoya's Z index [18,21,22] and the related Z_c index are obtained from the coefficients of the matching and characteristic polynomials as defined by:

$$Z = (\sum |a_k|)$$

$$Z_c = (\sum |C_k|)$$

As both Z and Z_c grow astronomically, and in order to make them comparable to our delta aromatic indices, we introduce two indices using the scaled natural logarithmic functions as follows:

$$\zeta_M = \frac{1}{n} \ln(\sum |a_k|)$$

$$\zeta_C = \frac{1}{n} \ln(\sum |C_k|)$$

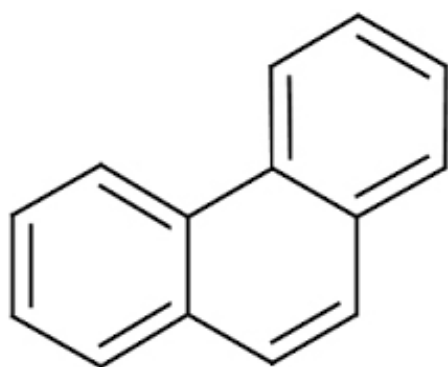
where the first zeta-index is obtained using the coefficients of the matching polynomial, while the second zeta-index is obtained from the coefficients of the characteristic polynomials. Consequently, we have four measures that can be computed and compared for different graphs. Among these, we have found that both regular and weighted delta indices are

good predictors of aromaticity and the relative order of aromaticity among a variety of compounds that we compare here.

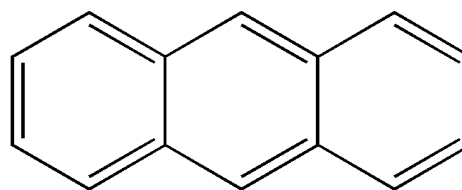
The characteristic polynomials of all structures were computed using the Frame method developed previously [71–74] while the matching polynomials were computed using a recursive pruning algorithm described in detail in previous studies [71–74]. We note that the philosophy behind the delta index in comparison to the zeta indices is that the zeta index derived from the matching polynomial includes only acyclic contributions while the zeta index obtained from the characteristic polynomial includes both cyclic and acyclic contributions without any differentiation. Therefore, the delta indices offer a compromise as they completely eliminate purely acyclic components. The other advantage of the delta indices is that unlike the topological resonance energy or bond energy or circuit energy computations that require the eigenvalues, the delta indices are easier to compute as they involve only the coefficients of the matching and characteristic polynomials. This is an advantage because for larger systems, the computations of all roots of the matching polynomials with reasonable accuracy could pose problems. It appears that the delta indices offer a reasonable compromise and yet they seem to closely mimic the aromaticity trends. It should be noted that the delta polynomials go to zero for trees or purely acyclic molecules, which is consistent with the fact that such compounds are not aromatic, and hence the delta indices are not defined for such purely acyclic molecules that are not aromatic. The next section describes the results of our computations and comparison of a number of polycyclic compounds with varied complexity, including three-dimensional structures such as fullerenes C_{60} and C_{70} .

3. Results and Discussion

We considered a number of structures with varied complexities for the study of delta polynomials and the zeta and delta aromatic indices of these structures. Figure 1 shows a compilation of such structures that were considered in this study. As seen from Figure 1, we included planar polycyclic compounds and three-dimensional spherical structures such as C_{60} , C_{70} and C_{72} , as well as polycyclic structures with holes, such as kekulene, septulene and a zigzag macrocycle containing 21 rings. Consequently, these structures offer quite a varied platform for the comparison of relative aromaticity on the basis of the various computed indices.

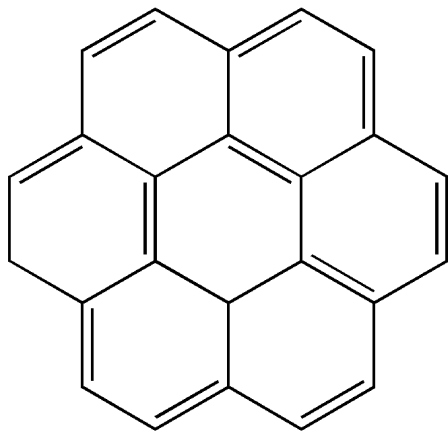


Phenanthrene

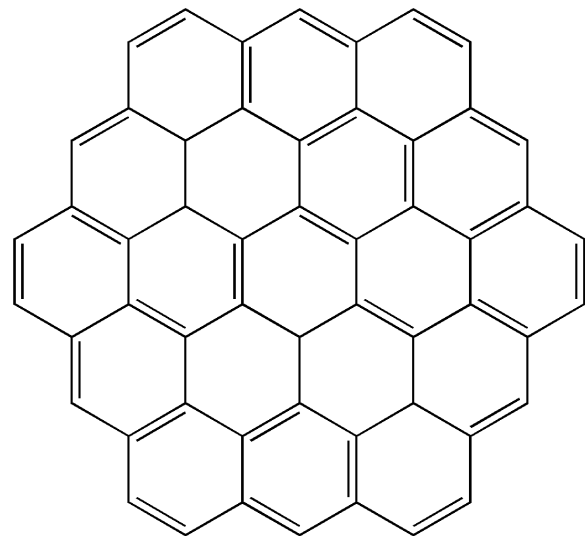


Anthracene

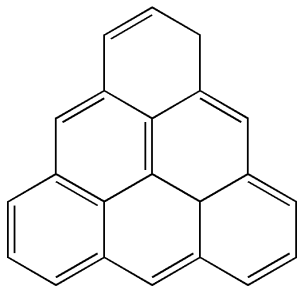
Figure 1. Cont.



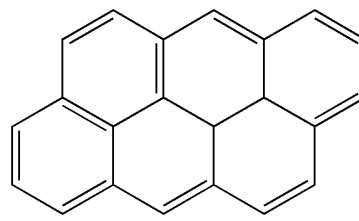
Coronene



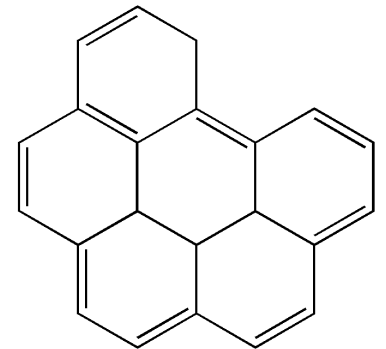
Circumcoronene



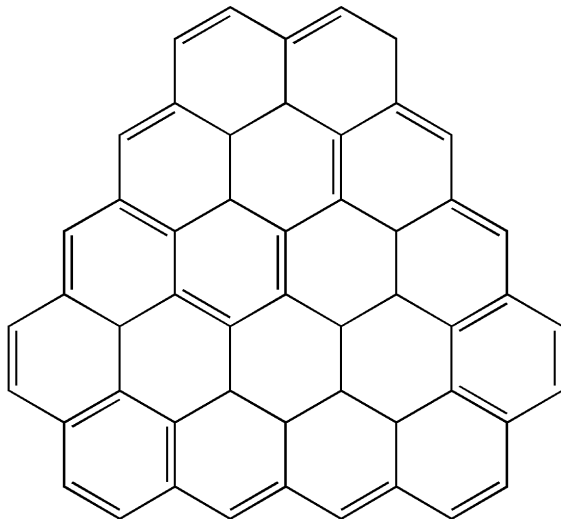
Triangulene



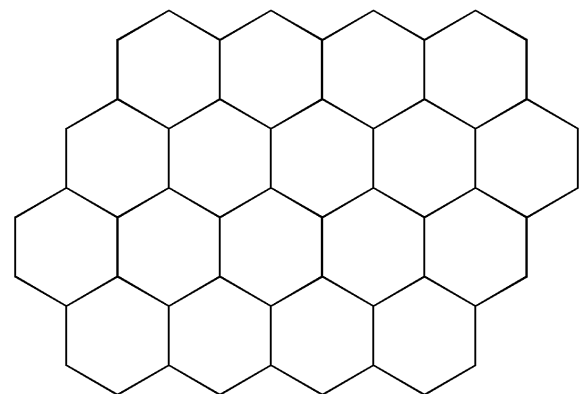
Anthraanthrene



Bezo[ghi]perylene

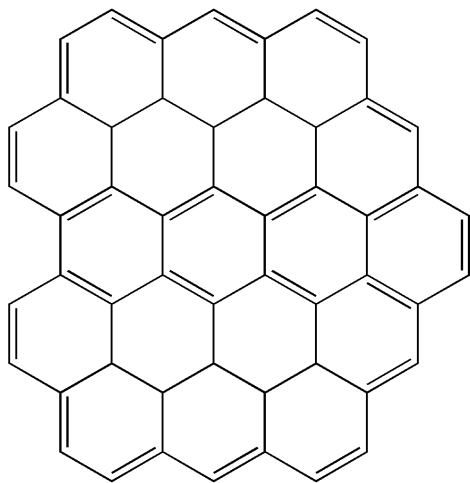


Circumtriangulene

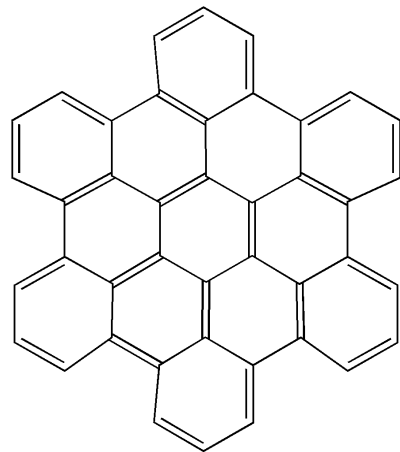


Circumanthraanthrene

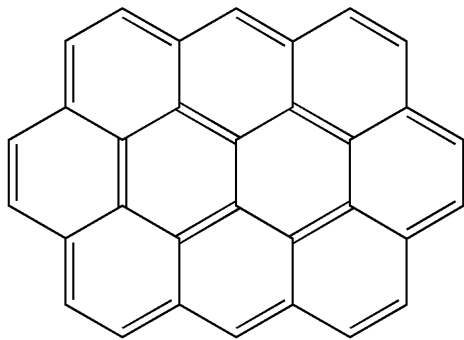
Figure 1. Cont.



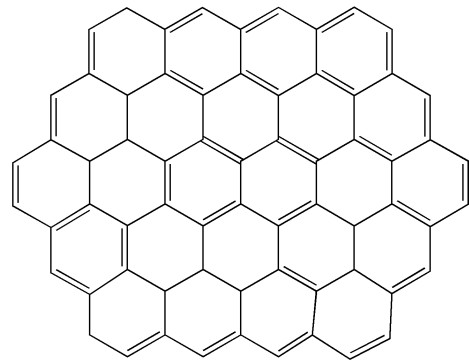
Circumbezo[ghi]perylene



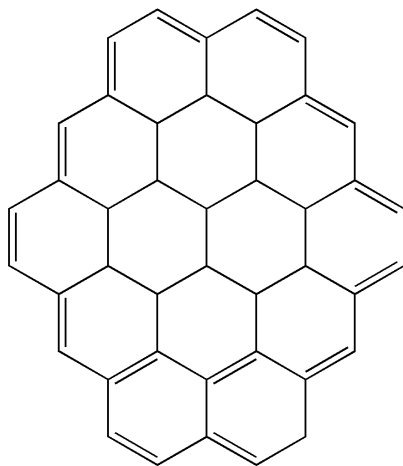
Hexabenzocoronene



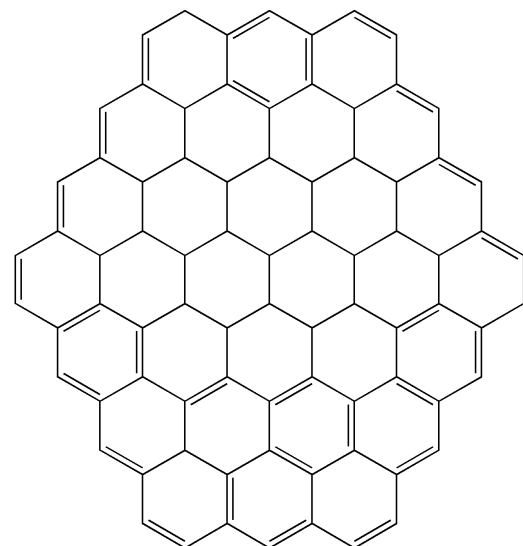
Ovalene



Circumovalene

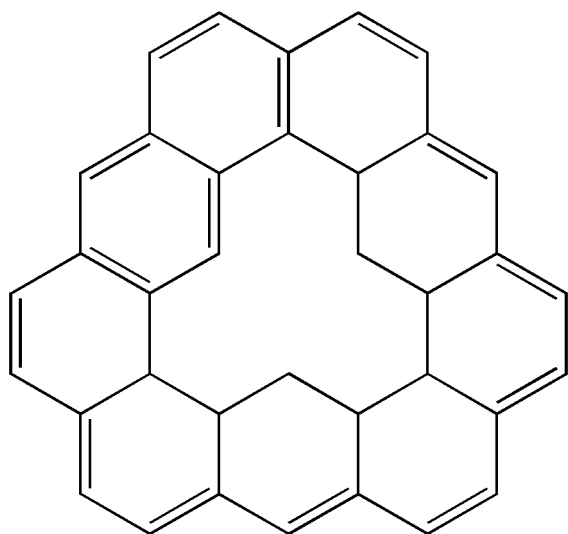


Circumpyrene

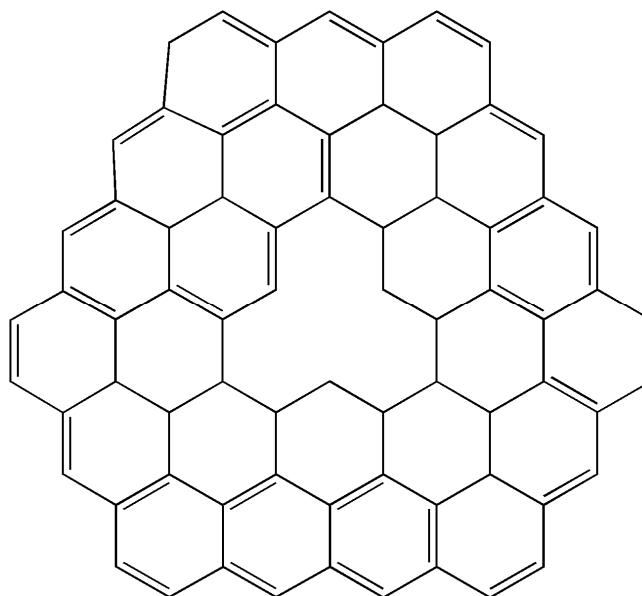


Circumcircumpyrene

Figure 1. Cont.



Coronaphene



Circumcoronaphene

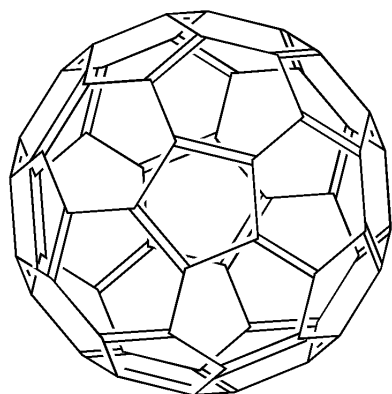
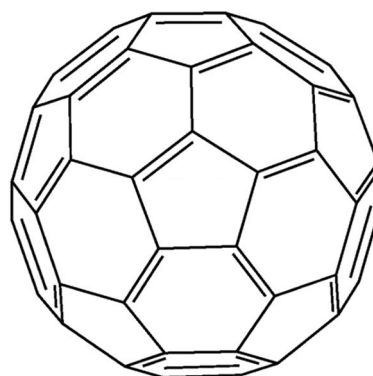
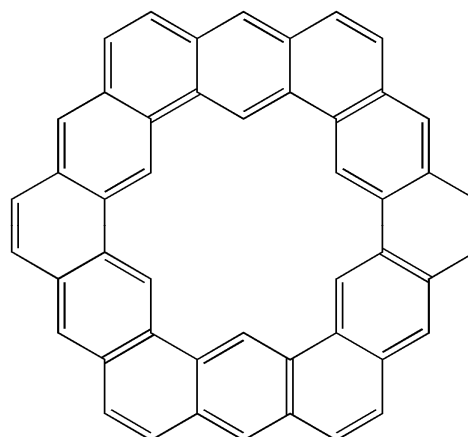
 $C_{60}(I_h)$  $C_{70}(D_{5h})$  $C_{72}(C_{2v})$ Kekulene(D_{6h})

Figure 1. Cont.

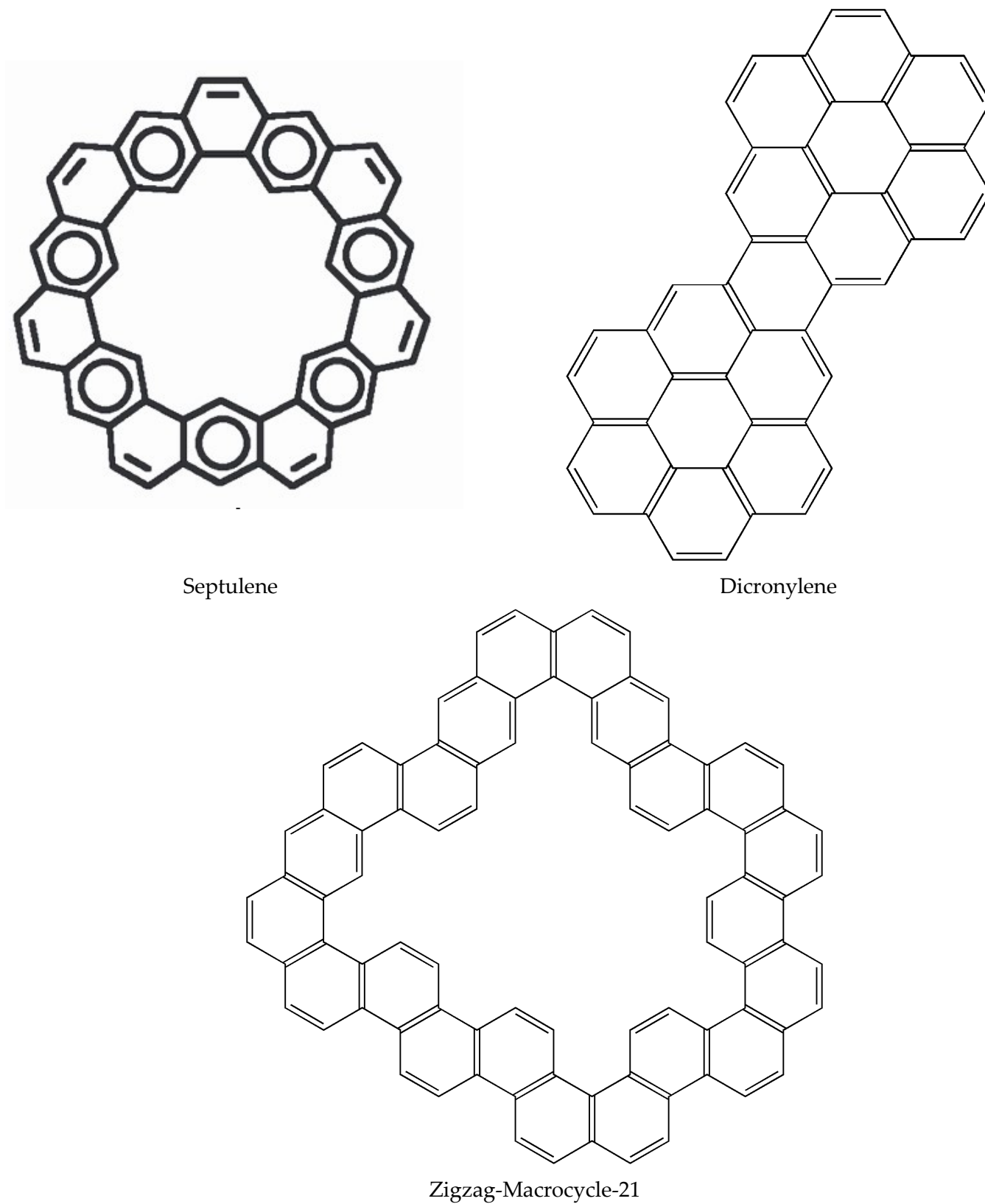


Figure 1. Structures of polycyclic compounds considered in this study. Not all displayed structures are meant to show any particular resonance/Clar's structure; the structures simply show the relationships and connectivities of various hexagonal rings.

Table 1 illustrates the computation of various aromatic indices; we have included the characteristic and matching polynomials of isomers of very simple structures with three benzene rings, that is, phenanthrene and anthracene. As can be seen from Table 1, as both are purely alternant benzenoids, as characterized by their bipartite graphs, the coefficients of the odd terms are zeroes. The constant term of the matching polynomial is simply the number of resonance structures, which is five for phenanthrene and four for anthracene, a well-known result, indicating that phenanthrene is more aromatic than anthracene. Herndon's [81] resonance energy is simply formulated as a scaled log of the number of resonance structures multiplied with a constant. However, we note that the constant term in the matching polynomial alone does not correlate with aromaticity or the stability of a structure. One needs to consider the contributions from various circuits, which are included in the other coefficients. The coefficients of other terms in the two polynomials yield the combinatorial numbers for other Sachs' subgraphs. The delta polynomials thus contain only non-acyclic terms enumerated among the Sachs' subgraphs, although some of the terms contain both disjoint circuits and dimers. The last but one row in Table 1 shows the sum of the coefficients of the characteristic polynomial, the sum of the coefficients of the matching polynomial, the well-known Hosoya's [18,22] Z index and, finally, the corresponding sums of delta polynomial coefficients. We also introduced a new weighted index concept that we designate as $\sum k\delta_k$, which weighs over different components of the Sachs' non-acyclic graphs. The philosophy behind this is that not all Sachs' circuits contained in different coefficients make the same contribution, and hence one needs to introduce weights as given by the total number of vertices in these disjointed circuits or simply k . For example, $k = 8$ would designate a circuit of length 8, a circuit of length 6 + a dimer, and so forth. Thus, by weighting the coefficients with k , we have taken this important factor into account, that is, not all coefficients have the same circuit lengths, and thus, the weighting method provides a means for contrasting their contributions. The last row shows the scaled natural logarithmic indices derived from these sums. First, the natural logarithmic functions reduces the astronomically large combinatorial numbers for the sums of these coefficients for large polycyclics. This, combined with a scaling method, in which we divide the natural logarithm by the number of vertices, eliminates the size dependency. Thus, the scaled logarithmic index provides a uniform basis to compare and contrast the aromaticity of a large number of polycyclic compounds with varied sizes and complexities. Therefore, as can be seen from Table 1, phenanthrene has scaled zeta and delta indices of ζ_C : 0.5218471, ζ_M : 0.5083718, Δ : 0.3960841 and Δ_W : 0.5642518, while the corresponding indices for anthracene are ζ_C : 0.5194570, ζ_M : 0.5069087, Δ : 0.3890527 and Δ_W : 0.5559446. It was noted that the indices reveal a contrast between phenanthrene and anthracene and predict a correct trend of aromaticity. However, in general cases, as the Hosoya index is derived from purely acyclic or dimer terms, while aromaticity involves circuits, delta indices, especially in the weighted forms, offer a good measure of aromaticity. This is especially true when a comparison needs to be made for compounds of varied sizes and complexities. All techniques lead to the same conclusion that phenanthrene is more aromatic than anthracene, as expected. We also obtained the delta polynomials of a number of zigzag and linear polyacenes of larger sizes. The general trend is that the weighted delta index is larger for the zigzag structures compared to linear polyacenes, which is consistent with the trend that the zigzag polyacenes are more aromatic than linear polyacenes. This arises from a Fibonacci increase in the resonance count for each kink in the structure of a zigzag polyacene. This in turn translates into a larger weighted delta index for a zigzag polycyclic as compared with a linear polyacene.

Table 1. Characteristic, matching and delta polynomials of phenanthrene and the derived Z, zeta and delta indices.

Phenanthrene			
n – k	Characteristic Polynomial	Matching Polynomial	Delta Polynomial
14	1.0	1.0	0.0
13	0.0	0.0	0.0
12	–16.0	–16.0	0.0
11	0.0	0.0	0.0
10	98.0	98.0	0.0
9	0.0	0.0	0.0
8	–297.0	–291.0	6.0
7	0.0	0.0	0.0
6	479.0	435.0	44.0
5	0.0	0.0	0.0
4	–407.0	–305.0	102.0
3	0.0	0.0	0.0
2	166.0	82.0	84.0
1	0.0	0.0	0.0
0	–25.0	–5.0	20.0
Z _C : 1489	Z: 1233	$\sum \delta_k = 256$	$\sum k\delta_k = 2696$
ζ_C : 0.5218471	ζ_M : 0.5083718	Δ : 0.3960841	Δ_W : 0.5642518
Anthracene			
n – k	Characteristic Polynomial	Matching Polynomial	Delta Polynomial
14	1	1	0
13	0	0	0
12	–16	–16	0
11	0	0	0
10	98	98	0
9	0	0	0
8	–296	–290	6
7	0	0	0
6	473	429	44
5	0	0	0
4	–392	–294	98
3	0	0	0
2	148	76	72
1	0	0	0
0	–16	–4	12
Z _C : 1440	Z: 1208	$\sum \delta_k = 232$	$\sum k\delta_k = 2400$
ζ_C : 0.5194570	ζ_M : 0.5069087	Δ : 0.3890527	Δ_W : 0.5559446

The two simple cases are considered for illustrative purposes only, as we demonstrate the power of the techniques with more complex polycyclics starting with coronene and circumcoronene. The computed results for these two structures are shown in Tables 2 and 3, respectively. As seen from these tables, the first several terms of the delta polynomials are zeroes, as these terms contain only purely acyclic contributions. For coronene, the first non-zero term in the delta polynomial corresponds to the seventh term, which contains the contributions of from a hexagon in the structure, and since there are no four-membered rings in the structure, only hexagons make contributions to this term. Starting with this term, all other subsequent terms contain various other types of circuits in the structure together with contributions from some disjoint dimers. Consequently, the unweighted delta indices computed from the coefficients of the delta polynomial are 0.4897992 and 0.5482407, respectively, clearly suggesting that circumscribing coronene results in considerably enhanced aromaticity. The constant coefficients of the two matching polynomials are given by 20 and 980, respectively, which are also the well-known Kekulé counts of the two structures. As these are purely alternant benzenoid polycyclic aromatic compounds, the square of the constant coefficients in the matching polynomials yields the constant coefficients in the characteristic polynomial. We shall discuss in a subsequent paragraph the weighted delta index together with the other indices of all polycyclics considered in this study. Table 4 shows the various polynomials obtained for kekulene together with the corresponding unweighted zeta and delta indices. Kekulene can be generated by the circumcision of the central hexagon of the coronene structure. Consequently, when one compares the unweighted delta indices of the two structures, one can infer that circumcision results in a lower delta index for kekulene compared to coronene. That is, circumcision disrupts the various circuits that were present in coronene, resulting in a lower π -electronic ring current or lower aromaticity in kekulene compared to coronene. This feature is mirrored by the delta indices of the two structures.

Tables 5 and 6 consider three polycyclic isomers of $C_{22}H_{12}$ and the corresponding circumscribed structures of the three isomers, respectively. The three isomers have been enumerated in the handbook by Dias [57] on polycyclic aromatic compounds. The three isomers, namely, triangulene, anthanthrene and benzo[ghi]perylene, represent interesting cases for our study. Among these, triangulene exhibits a triplet electronic ground state and it is thus a diradical. We note that this is directly inferred by the zero coefficient of the constant term of the characteristic polynomial of triangulene, consistent with a doubly degenerate set of HOMOs, resulting in a triplet ground state. As seen from Table 5, the delta indices of the three structures indicate that benzo[ghi]perylene is the most aromatic of the three structures with triangulene being the least aromatic. Although the combinatorial numbers in Table 6 become more complex due to a greater number of various circuits in the corresponding circumscribed structures, the final delta indices are much more amenable to critical comparison and thus shed light on the potential aromaticity of these compounds. Again, comparing the delta indices of the primitive and circumscribed counterparts in Tables 5 and 6 reveals that circumscribing results in greater aromaticity compared to the uncircumscribed structure. The gaps relative to aromaticity among the isomers are narrowed somewhat when one compares the circumscribed structures to their uncircumscribed counterparts. In particular, triangulenes obtain a greater aromaticity upon circumscribing. However, we note that better measures are obtained using the weighted delta indices which we compare in a subsequent Table and paragraph. Furthermore, as seen from Table 6, the constant coefficient of the circumscribed triangulene continues to be zero for the characteristic polynomial suggesting that circumtriangulene continues to exhibit a triplet diradical ground state although its aromaticity is enhanced relative to the primitive triangulene structure. This trend is repeated by a number of structures that we have tested and are not shown here. The general trend is that circumscribing a given structure results in enhanced aromaticity while circumcision results in lower aromaticity.

Table 2. Characteristic, matching and delta polynomials of coronene.

$n - k$	Char. Poly.	Match. Poly.	Delta Poly.
24	1	1	0
23	0	0	0
22	−30	−30	0
21	0	0	0
20	387	387	0
19	0	0	0
18	−2832	−2818	14
17	0	0	0
16	13059	12783	276
15	0	0	0
14	−39858	−37620	2238
13	0	0	0
12	82281	72585	9696
11	0	0	0
10	−115272	−90792	24480
9	0	0	0
8	108192	71256	36936
7	0	0	0
6	−65864	−32968	32896
5	0	0	0
4	24432	8016	16416
3	0	0	0
2	−4896	−816	4080
1	0	0	0
0	400	20	380
$\sum x_k ^a$	457504	330092	127412
$\frac{1}{n} \ln(\sum x_k)$	0.5430642	0.5294636	0.4897992

^a x_k designates the coefficient in the respective polynomial (characteristic or matching or delta polynomial) of the corresponding column.

Table 3. Characteristic, matching and delta polynomials of circumcoronene.

$n - k$	Char. Poly.	Match. Poly.	Delta Poly.
54	1	1	0
53	0	0	0
52	−72	−72	0
51	0	0	0
50	2430	2430	0
49	0	0	0
48	−51152	−51114	38
47	0	0	0

Table 3. Cont.

n – k	Char. Poly.	Match. Poly.	Delta Poly.
46	753867	751551	2316
45	0	0	0
44	–8277552	–8211876	65676
43	0	0	0
42	70356380	69204580	1151800
41	0	0	0
40	–474823692	–460817112	14006580
39	0	0	0
38	2589615333	2464100913	125514420
37	0	0	0
36	–11556300564	–10696440044	859860520
35	0	0	0
34	42569538372	37958165700	4611372672
33	0	0	0
32	–130222965528	–110557089534	19665875994
31	0	0	0
30	332069146453	264687311485	67381834968
29	0	0	0
28	–707192500956	–520523395944	186669105012
27	0	0	0
26	1257989920284	838506886932	419483033352
25	0	0	0
24	–1866287443412	–1101123547848	765163895564
23	0	0	0
22	2301545596335	1170542244231	1131003352104
21	0	0	0
20	–2347222219224	–997848645108	1349373574116
19	0	0	0
18	1965105336102	673809199342	1291296136760
17	0	0	0
16	–1337106330756	–354768478638	982337852118
15	0	0	0
14	729597602706	142707108690	586890494016
13	0	0	0
12	–313604239964	–42704574172	270899665792
11	0	0	0
10	103654073940	9173052348	94481021592
9	0	0	0
8	–25479629340	–1345586058	24134043282
7	0	0	0

Table 3. Cont.

$n - k$	Char. Poly.	Match. Poly.	Delta Poly.
6	4438832481	125224733	4313607748
5	0	0	0
4	−508728588	−6568740	502159848
3	0	0	0
2	33696516	156144	33540372
1	0	0	0
0	−960400	−980	959420
$\sum x_k $	13479328942400	6280086816320	7199242126080
$\frac{1}{n} \ln(\sum x_k)$	0.5598552	0.5457112	0.5482407

Table 4. Characteristic, matching and delta polynomials of kekulene.

$n - k$	Char. Poly.	Match. Poly.	Delta Poly.
48	1	1	0
47	0	0	0
46	−60	−60	0
45	0	0	0
44	1674	1674	0
43	0	0	0
42	−28874	−28850	−24
41	0	0	0
40	345327	344127	1200
39	0	0	0
38	−3044574	−3016998	27576
37	0	0	0
36	20538689	20152013	386676
35	0	0	0
34	−108618240	−104913492	3704748
33	0	0	0
32	457707249	431969433	25737816
31	0	0	0
30	−1553676412	−1419382254	134294158
29	0	0	0
28	4277976000	3740060904	537915096
27	0	0	0
26	−9591327648	−7914718788	1676608860
25	0	0	0
24	17529851809	13431639205	4098212604
23	0	0	0
22	−26083608096	−18200982024	7882626072

Table 4. Cont.

$n - k$	Char. Poly.	Match. Poly.	Delta Poly.
21	0	0	0
20	31479717969	19552772649	11926945320
19	0	0	0
18	-30623699358	-16479660654	14144038704
17	0	0	0
16	23797431375	10743316299	13054115076
15	0	0	0
14	-14592392910	-5315219724	9277173186
13	0	0	0
12	6947150082	1945680262	5001469820
11	0	0	0
10	-2513544072	-509172702	2004371370
9	0	0	0
8	671549841	90806961	580742880
7	0	0	0
6	-127206956	-10292946	116914010
5	0	0	0
4	16035984	665136	15370848
3	0	0	0
2	-1198800	-20328	1178472
1	0	0	0
0	40000	200	39800
$\sum x_k $	170396692000	99914817684	70481874316
$\frac{1}{n} \ln(\sum x_k)$	0.5387791	0.5276580	0.5203879

Table 5. Characteristic, matching and delta polynomials of three polycyclic isomers of C₂₂H₁₂.

$n - k$	Characteristic Polynomials			Matching Polynomials			Delta Polynomials		
	Triangulene	Anthanthrene	Bezo[ghi]Perylene	Triangulene	Anthanthrene	Bezo[ghi]Perylene	Triangulene	Anthanthrene	Bezo[ghi]Perylene
22	1	1	1	1	1	1	0	0	0
21	0	0	0	0	0	0	0	0	0
20	-27	-27	-27	-27	-27	27	0	0	0
19	0	0	0	0	0	0	0	0	0
18	309	309	309	309	309	309	0	0	0
17	0	0	0	0	0	0	0	0	0
16	-1973	-1973	-1974	-1961	-1961	1962	12	12	-12
15	0	0	0	0	0	0	0	0	0
14	7782	7783	7800	7578	7579	7596	204	204	204
13	0	0	0	0	0	0	0	0	0
12	-19818	-19831	-19953	-18426	-18441	18557	1392	1390	-1396
11	0	0	0	0	0	0	0	0	0
10	33027	33110	33580	28127	28218	28624	4900	4892	4956
9	0	0	0	0	0	0	0	0	0
8	-35619	-35902	-36968	-26079	-26354	27126	9540	9548	-9842

Table 5. Cont.

n – k	Characteristic Polynomials			Matching Polynomials			Delta Polynomials		
	Triangulene	Anthanthrene	Bezo[ghi]Perylene	Triangulene	Anthanthrene	Bezo[ghi]Perylene	Triangulene	Anthanthrene	Bezo[ghi]Perylene
7	0	0	0	0	0	0	0	0	0
6	23853	24400	25864	13659	14086	14866	10194	10314	10998
5	0	0	0	0	0	0	0	0	0
4	–8987	–9609	–10796	–3491	–3817	4202	5496	5792	–6594
3	0	0	0	0	0	0	0	0	0
2	1452	1840	2360	306	414	490	1146	1426	1870
1	0	0	0	0	0	0	0	0	0
0	0	–100	–196	0	–10	14	0	90	–182
$\sum x_k $	132848	134885	139828	99964	101217	103774	32884	33668	36054
$\frac{1}{n} \ln(\sum x_k)$	0.5362255	0.5369172	0.5385531	0.5232984	0.5238646	0.5249987	0.4727610	0.4738320	0.4769442

Table 6. Characteristic, matching and delta polynomials of three circumscribed isomers: C₅₂H₁₇, circumtriangulene, circumanthanthrene and Circumbezo[ghi] perylene.

Circumtriangulene			Circumanthanthrene			Circumbezo[ghi] Perylene					
n – k	Characteristic Polynomial	Matching Polynomial	Delta Polynomial	n – k	Characteristic Polynomial	Matching Polynomial	Delta Polynomial	n – k	Characteristic Polynomial	Matching Polynomial	Delta Polynomial
52	1	1	0	52	1	1	0	52	1	1	0
51	0	0	0	51	0	0	0	51	0	0	0
50	–69	–69	0	50	–69	–69	0	50	–69	–69	0
49	0	0	0	49	0	0	0	49	0	0	0
48	2226	2226	0	48	2226	2226	0	48	2226	2226	0
47	0	0	0	47	0	0	0	47	0	0	0
46	–44668	–44632	36	46	–44668	–44632	36	46	–44669	–44633	36
45	0	0	0	45	0	0	0	45	0	0	0
44	625713	623625	2088	44	625713	623625	2088	44	625772	623684	2088
43	0	0	0	43	0	0	0	43	0	0	0
42	–6509829	–6453663	56166	42	–6509829	–6453663	56166	42	–6511448	–6455276	56172
41	0	0	0	41	0	0	0	41	0	0	0
40	52251216	51320120	931096	40	52251217	51320121	931096	40	52278690	51347258	931432
39	0	0	0	39	0	0	0	39	0	0	0
38	–331796412	–321134574	10661838	38	–331796457	–321134625	10661832	38	–332119812	–321449318	10670494
37	0	0	0	37	0	0	0	37	0	0	0
36	1695928914	1606342218	89586696	36	1695929871	1606343417	89586454	36	1698736514	1609013576	89722938
35	0	0	0	35	0	0	0	35	0	0	0
34	–7062439782	–6489636480	572803302	34	–7062452491	–6489653683	572798808	34	–7081100003	–6506829077	574270926
33	0	0	0	33	0	0	0	33	0	0	0
32	24162689001	21310401549	2852287452	32	24162806822	21310569758	2852237064	32	24259975217	21396200135	2863775082
31	0	0	0	31	0	0	0	31	0	0	0
30	–68292453531	–57062874051	11229579480	30	–68293262612	–57064060212	11229202400	30	–68696889063	–57399597701	11297291362
29	0	0	0	29	0	0	0	29	0	0	0
28	159962255377	124669968135	35292287242	28	159966519220	124676198180	35290321040	28	161317740165	125718050333	3559689832
27	0	0	0	27	0	0	0	27	0	0	0
26	–310866022785	–221836072383	89029950402	26	–310883651811	–221860905503	89022746308	26	–314554717782	–224434299008	90120418774
25	0	0	0	25	0	0	0	25	0	0	0
24	500842466118	320162665770	180679800348	24	500900434871	320238551209	180661883662	24	509025810275	325296517073	183729293202
23	0	0	0	23	0	0	0	23	0	0	0
22	–667151021522	–372336242084	294814779438	22	–667303817619	–372514716699	294789100920	22	–681972062692	–380402520082	301569542610
21	0	0	0	21	0	0	0	21	0	0	0
20	731241744267	345720833133	385520911134	20	731565732441	346043561601	385522170840	20	753133601175	355744657295	397388943880
19	0	0	0	19	0	0	0	19	0	0	0
18	–654769892103	–253153062357	401616829746	18	–655322555267	–253599322123	401723233144	18	–681052897827	–262920853285	418132044542
17	0	0	0	17	0	0	0	17	0	0	0
16	474141118603	143835845437	330305273166	16	474897139634	144303164122	330593975512	16	499638000612	151208688842	348429311770

Table 6. Cont.

Circumtriangulene			Circumanthanthrene			Circumbezo[ghi] Perylene					
n – k	Characteristic Polynomial	Matching Polynomial	Delta Polynomial	n – k	Characteristic Polynomial	Matching Polynomial	Delta Polynomial	n – k	Characteristic Polynomial	Matching Polynomial	Delta Polynomial
15	0	0	0	15	0	0	0	15	0	0	0
14	–273813286767	–62077156797	211736129970	14	–274637349199	–62442496421	212194852778	14	–293623626123	–66316204751	227307421372
13	0	0	0	13	0	0	0	13	0	0	0
12	123696211872	19781999232	103914212640	12	124404621068	19991050046	104413571022	12	135872791533	21597079779	114275711754
11	0	0	0	11	0	0	0	11	0	0	0
10	–42539488824	–4477460040	38062028784	10	–43012391338	–4562686358	38449704980	10	–48360491101	–5038874031	43321617070
9	0	0	0	9	0	0	0	9	0	0	0
8	10698149700	680855244	10017294456	8	10937560349	704696745	10232863604	8	12811571672	801125198	12010446474
7	0	0	0	7	0	0	0	7	0	0	0
6	–1845219852	–63837084	1781382768	6	–1933743487	–68166823	1865576664	6	–2408005299	–80628339	2327376960
5	0	0	0	5	0	0	0	5	0	0	0
4	194068224	3177510	190890714	4	216497569	3644565	212853004	4	297960317	4566433	293393884
3	0	0	0	3	0	0	0	3	0	0	0
2	–9335088	–59886	9275202	2	–12786256	–85352	12700904	2	–21276306	–117326	21158980
1	0	0	0	1	0	0	0	1	0	0	0
0	0	0	0	0	240100	490	239610	0	648025	805	647220
$\sum x_k $	4053375022464	1955648068300	2097726954164	$\sum x_k $	4057600722205	1957859452269	2099741269936	$\sum x_k $	4196219484388	2006855745534	2189363738854
$\frac{1}{H} \ln(\sum x_k)$	0.5582802	0.5442643	0.5456130	$\frac{1}{H} \ln(\sum x_k)$	0.5583002	0.5442860	0.5456314	$\frac{1}{H} \ln(\sum x_k)$	0.5589463	0.5447614	0.5464352

Next, we consider three-dimensional and other structures that appear to exhibit aromatic characters or unusual stabilities. The celebrated buckminsterfullerene with the icosahedral I_h group has been the cynosure of fullerenes. Table 7 displays all three polynomials of C_{60} together with the sums of the columns and the scaled natural log indices. There are several differences that should be noted in the polynomials for the C_{60} structure compared to the other polycyclics that we have considered thus far. None of the coefficients of the odd terms except the first two odd terms is zero for the characteristic and delta polynomials of C_{60} . For example, the sixth or fifth coefficient, not counting the first term, is twenty-four for the delta polynomial and is consistent with the twelve pentagons present in the structure. Likewise, all other odd terms are non-zeroes and contribute toward the delta polynomial. This is a striking contrast compared to alternant benzenoid hydrocarbons. Furthermore, the square of the constant term in the matching polynomial does not yield the constant term of the characteristic polynomial. These features, together with several non-zero odd terms in the delta polynomials, provide C_{60} with some unique features. Although the sum of all the coefficients of the delta polynomial is 2508935631291784, a large number, the scaled log of the corresponding result is 0.5909773, suggesting that its unweighted delta aromaticity is much higher than the circumcoronene value of 0.5482407 and even circumcircumcoronene, circumkekulene and so forth. The weighted delta aromatic indices yield further insights, as we will now discuss. These results of C_{60} can also be compared with the corresponding indices of other fullerenes, such as $C_{70}(D_{5h})$ and $C_{72}(C_{2v})$, as shown below.

Table 7. Characteristic, matching and delta polynomials of C_{60} buckminsterfullerene.

n – k	Characteristic Polynomial	Matching Polynomial	Delta Polynomial
60	1	1	0
59	–0	0	0
58	–90	–90	0
57	–0	0	0
56	3825	3825	0

Table 7. Cont.

n – k	Characteristic Polynomial	Matching Polynomial	Delta Polynomial
55	–24	0	24
54	–102160	–102120	40
53	1920	0	1920
52	1925160	1922040	3120
51	–72240	0	72240
50	–27244512	–27130596	113916
49	1700640	0	1700640
48	300906380	298317860	2588520
47	–28113600	0	28113600
46	–2661033600	–2619980460	41053140
45	347208896	0	347208896
44	19180834020	18697786680	483047340
43	–3327625680	0	3327625680
42	–114118295000	–109742831260	4375463740
41	25376437920	0	25376437920
40	565407465144	534162544380	31244920764
39	–156652575440	0	156652575440
38	–2346799508400	–2168137517940	178661990460
37	792175427520	0	792175427520
36	8189116955350	7362904561730	826212393620
35	–3308173115904	0	3308173115904
34	–24056403184260	–20949286202160	3107116982100
33	11466942645600	0	11466942645600
32	59443188508110	4992488988850	9518298619260
31	–33076275953760	0	33076275953760
30	–123163094844616	–99463457244844	23699637599772
29	79417625268960	0	79417625268960
28	212712221820840	165074851632300	47637370188540
27	–158412719276240	0	158412719276240
26	–303315997028160	–227043126274260	76272870753900
25	261359090670624	0	261359090670624
24	351861389316780	256967614454320	94893774862460
23	–354145195147200	0	354145195147200
22	–324375523213200	–237135867688980	87239655524220
21	390055074762240	0	390055074762240
20	228227031040884	176345540119296	51881490921588
19	–344185906596720	0	344185906596720
18	–112654402736360	–104113567937140	8540834799220

Table 7. Cont.

$n - k$	Characteristic Polynomial	Matching Polynomial	Delta Polynomial
17	238553091055200	0	238553091055200
16	29617003666920	47883826976580	18266823309660
15	−126428882536240	0	126428882536240
14	4679380503120	−16742486291340	12063105788220
13	49433493646080	0	49433493646080
12	−8131429397135	4310718227685	3820711169450
11	−13627897407360	0	13627897407360
10	3576552321006	−783047312406	2793505008600
9	2527365617120	0	2527365617120
8	−831616531095	94541532165	737074998930
7	−310065067080	0	310065067080
6	108565938200	−6946574300	101619363900
5	26034025632	0	26034025632
4	−7440712560	269272620	7171439940
3	−1566501120	0	1566501120
2	186416640	−4202760	182213880
1	54743040	0	54743040
0	2985984	12500	2973484
$\sum x_k $	3865312407639512	1417036634543488	2508935631291784
$\frac{1}{n} \ln(\sum x_k)$	0.5981803	0.5814557	0.5909773

These computations can be extended to large macrocycles, such as the one shown in Figure 1 containing 21 hexagons arranged in a zigzag fashion with a large internal cavity. The various polynomials for such a macrocycle are shown in Table 8. As this is an alternant benzenoid hydrocarbon, we show only the coefficients of the even terms as all odd terms have zero coefficients for all three polynomials. This macrocycle with a zigzag structure has a delta index of 0.5352335, making it comparable to circumcoronene, which has a delta index of 0.5482407. This implies that the zigzag macrocycle with 21 rings is less aromatic compared to circumcoronene but more aromatic compared to kekulene with a delta index of 0.5203879. We note that the weighted delta index appears to provide yet another reliable way to compare different structures, although any of these indices should be used in conjunction with other parameters, such as the HOMO-LUMO gap or electronic or magnetic parameters derived from quantum chemical computations.

Table 8. Characteristic, matching and delta polynomials of the zigzag macrocycle-21 together with their indices.

$n - k$	C_k	M_k	δ_k
84	1	1	0
82	−105	−105	0
80	5292	5292	0
78	−170552	−170510	42
76	3950629	3946639	3990

Table 8. Cont.

$n - k$	C_k	M_k	δ_k
74	−70093203	−69911859	181344
72	991282749	986031143	5251606
70	−11482348005	−11373459253	108888752
68	111090087176	109367937824	1722149352
66	−910947963808	−889334531796	21613432012
64	6402925439287	6181826617949	221098821338
62	−38919293230683	−37040011262025	1879281968658
60	206013904397115	192551488336995	13462416060120
58	−955002794104467	−872839129452669	82163664651798
56	3894336217341121	3463521386236771	430814831104350
54	−14019373614031827	−12066034271467827	1953339342564000
52	44678801369930336	36981548810147848	7697252559782488
50	−126321154074068661	−99857114193811115	26464039880257546
48	317338685795324123	237720042560254363	79618643235069760
46	−709062372660591571	−49906339626984227	210056033033607344
44	1409909022006755539	923239449763670729	486669572243084810
42	−2495016469484972200	−1504059185145959400	990957284339012800
40	3927963303866069473	2154224942879036951	1773738360987032522
38	−5496873577643855036	−2706936481872745914	2789937095771109122
36	6829111016615764029	2976116960372998897	3852994056242765132
34	−7518883235006766618	−2853311058653127710	4665572176353638908
32	7319902384178141972	2375786868595946840	4944115515582195132
30	−6283532923932044803	−1709655914472694895	4573877009459349908
28	4739885867813791187	1057153335134041467	3682732532679749720
26	−3129063398676383265	−557849001975167171	2571214396701216094
24	1798911321678387099	249182267286144541	1549729054392242558
22	−895371948756710388	−93314898694188010	802057050062522378
20	383122049845443519	28961471055606009	354160578789837510
18	−139739031770502510	−7347157054733772	132391874715768738
16	42996786829876846	1498155252911156	41498631576965690
14	−11017873944937905	−240532059951131	10777341884986774
12	2313181667668728	29633110868332	2283548556800396
10	−389499119207522	−2710827868354	386788291339168
8	51095415744876	176380210708	50919035534168
6	−5008008625962	−7697442472	5000311183490
4	343396584009	206946163	343189637846
2	−14620716108	−2982916	14617733192
0	289340100	17014	289323086
$\sum x_k $	53640581451802650405	20089114432935826763	33551467018866823642
$\frac{1}{n} \ln(\sum x_k)$	0.5408195	0.5291275	0.5352335

Table 9 shows a cumulative across-board comparison of all four indices of all structures that are considered in the present study. As both delta and zeta indices are derived from scaled natural log values, we uniformly multiplied the indices by a factor of 10 in Table 9 for comparison. It can be seen from Table 9 that the weighted delta index appears to provide one of the best measures of aromaticity and stability. For example, the weighted delta index of buckminsterfullerene stands out as 6.516865, a maximum among all structures considered here with the exception of graphene. In fact, while the weighted delta index of buckminsterfullerene is higher than both $C_{70}(D_{5h})$ and $C_{72}(C_{2v})$, this trend is not reproduced by any of the other indices shown in Table 9. We note that both $C_{72}(C_{2v})$ and $C_{72}(D_{6d})$ structures have been found to be stable isomers [82,83]. Moreover, we note that as the weighted delta indices do not vary in large magnitude, and small changes should be considered important as the weighted indices are subtle in their variations. As seen from Table 9, circumcoronene is more aromatic than coronene as well as hexbenzcoronene. Polycyclic structures with cavities, such as coronaphene, circumcoronaphene, kekulene, etc., are less aromatic compared to their parent structures prior to circumcision. On the other hand, kekulene and septulene have a remarkably similar aromaticity, as inferred from their weighted delta indices of 5.914023 and 5.884901, respectively. Of the three $C_{22}H_{12}$ isomers, triangulene exhibits the least aromaticity while benzo[ghi]perylene exhibits the greatest aromaticity. We also note a few variations in trends, for example, ovalene is predicted to be much less aromatic compared to circumovalene on the basis of zeta and unweighted delta index but the weighted delta index exhibits the same trend but with a smaller contrast. While circumpyrene is predicted to be less aromatic compared to circumovalene on the basis of the zeta and unweighted delta indices, the weighted delta index predicts the opposite trend with a smaller contrast.

Kekulene and septulene are virtually identical relative to the zeta indices, as can be seen from Table 9. The identical values of the scaled Hosoya index require further inquiry. Moreover, the delta index suggests an opposite trend, in that it predicts septulene to be slightly more aromatic compared to kekulene, although the weighted delta index predicts kekulene to be slightly more aromatic than septulene. The sum of the coefficients of the three polynomials and the weighted sum for kekulene are given as 170396692000, 99914817684, 70481874316 and 2130357387264, respectively. The corresponding values for septulene are 12686887009024, 6806150529706, 5880736479318 and 205289991176192, respectively. Consequently, although these numbers are quite different for kekulene and septulene, when they are scaled by the number of vertices after taking log of these values, accidental degeneracy is reached for kekulene relative to Hosoya's Z index while the Z_c index is almost the same. Thus, these two indices fail to differentiate septulene and kekulene while the weighted delta index appears to provide the correct trend.

We were able to obtain an estimate of the aromaticity delta index for graphene using an extrapolation scheme by using the results of coronene, circumcoronene and circumcircumcoronene. A previous study on the degree-based topological indices of series of polycyclic aromatics [69] has revealed that if one extrapolates the results of known circumcoronene series with the order of circumscribing as $n \sim 6.4$, one obtains the results converging to graphene. By using the same extrapolation scheme with the results obtained for coronene, circumcoronene and circumcircumcoronene, we obtain the weighted and unweighted delta indices for graphene converging to 6.77. Consequently, one can compare this value to C_{60} value of 6.516865 and conclude that the correct trend is predicted by the newly formulated delta aromatic indices and delta polynomials. Indeed, the highly symmetric buckminsterfullerene is confirmed to be the most stable species among small molecules, fullerenes, and clusters, which corroborates with experimental observations. Furthermore, we note that other topological indices have been applied to different forms of carbon and other complex networks such as diamond and other metal organic frameworks [84,85].

Table 9. Computed zeta and delta aromatic indices of polycyclic compounds.

System	$\zeta_C \times 10^{-1}$	$\zeta_M \times 10^{-1}$	$\Delta \times 10^{-1}$	$\Delta_W \times 10^{-1}$
Coronene	5.430642	5.294636	4.897992	6.064420
Circumcoronene	5.598552	5.457112	5.482407	6.137828
Hexbencoronene	5.520197	5.375805	5.332557	6.120283
Ovalene	5.489804	5.353347	5.165118	6.119007
Circumovalene	5.630656	5.487418	5.556126	6.121432
Circumpyrene	5.547669	5.408986	5.352999	6.139214
Circumcircumpyrene	5.661399	5.516115	5.614513	6.104184
Coronaphene	5.394510	5.281798	5.089506	5.963508
Circumcoronaphene	5.513583	5.452279	5.371723	5.903852
C ₆₀ (I _h)	5.981803	5.814557	5.909773	6.516865
C ₇₀ (D _{5h})	5.985028	5.814903	5.934508	6.476662
C ₇₂ (C _{2v})	5.986215	5.814966	5.939604	6.470739
Kekulene	5.387791	5.276580	5.203879	5.914023
Septulene	5.387784	5.276580	5.250483	5.884901
Dicronylene	5.510041	5.374743	5.356110	6.069668
Triangulene (C ₂₂ H ₁₂)	5.362255	5.232984	4.727610	5.958243
Anthanthrene (C ₂₂ H ₁₂)	5.369172	5.238646	4.738320	5.971711
Bezo[ghi]perylene (C ₂₂ H ₁₂)	5.385531	5.249987	4.769442	6.007196
Circumtriangulene (C ₅₂ H ₁₈)	5.582802	5.442643	5.456130	6.129567
Circumanthanthrene (C ₅₂ H ₁₈)	5.583002	5.442860	5.456314	6.129790
Circumbezo[ghi]perylene (C ₅₂ H ₁₈)	5.589463	5.447614	5.464352	6.138383
Macro-zig-21	5.408195	5.291275	5.352335	5.822065
Graphene			[6.771]	[6.77]

4. Conclusions

In this study, we proposed hybrid polynomials called delta polynomials and created two scaled logarithmic indices, which we called delta aromatic indices. These indices combined with the zeta indices, which are also scaled versions, were evaluated for a number of polycyclic structures, including fullerenes, kekulenes, septulene, circumcoronene, circumcoronaphene, dicronylene, macrocycles and different isomers of polycyclic compounds. It was shown that the delta indices, especially the weighted delta indices, appear to conform closely with the aromaticity trends of the investigated compounds. We suggest that these newly proposed delta indices can be used in conjunction with other topological, electronic, magnetic and quantum chemical parameters to gain considerable insights into the longstanding phenomenon of aromaticity, superaromaticity and spherical aromaticity.

Funding: This research received no external funding.

Data Availability Statement: All data used in this manuscript are contained in the manuscript.

Conflicts of Interest: The author declares no conflicts of interest.

References

1. Kroto, H.W.; Heath, J.R.; O'Brien, S.C.; Curl, R.F.; Smalley, R.E. C₆₀: Buckminsterfullerene. *Nature* **1985**, *318*, 162–163. [[CrossRef](#)]
2. Smalley, R.E. Discovering the fullerenes. *Rev. Mod. Phys.* **1997**, *69*, 723–730. [[CrossRef](#)]
3. Diederich, F.; Staab, H.A. Benzenoid versus Annulenoic Aromaticity: Synthesis and Properties of Kekulene. *Angew. Chem. Int. Ed. Engl.* **1978**, *17*, 372. [[CrossRef](#)]

4. Schweitzer, D.; Hausser, K.H.; Vogler, H.; Diederich, F.; Staab, H. Electronic Properties of Kekulene. *Mol. Phys.* **1982**, *46*, 1141–1153. [[CrossRef](#)]
5. Staab, H.A.; Diederich, F.; Krieger, C.; Schweitzer, D. Cycloarenes, a New Class of Aromatic Compounds, I. Synthesis of Kekulene. *Chem. Ber.* **1983**, *116*, 3. [[CrossRef](#)]
6. Kumar, B.; Viboh, R.L.; Bonifacio, M.C.; Thompson, W.B.; Buttrick, J.C.; Westlake, B.C.; Kim, M.; Zoellner, R.W.; Varganov, S.A.; Mörschel, P.; et al. Septulene: The heptagonal homologue of kekulenes. *Angew. Chem. Int. Ed.* **2012**, *51*, 12795–12800. [[CrossRef](#)] [[PubMed](#)]
7. Majewski, M.A.; Hong, Y.; Lis, T.; Gregoliński, J.; Chmielewski, P.J.; Cybińska, J.; Kim, D.; Stępień, M. Octulene: A Hyperbolic Molecular Belt that Binds Chloride Anions. *Angew. Chem. Int. Ed.* **2016**, *55*, 14072–14076. [[CrossRef](#)] [[PubMed](#)]
8. Wu, J.; Watson, M.D.; Zhang, L.; Wang, Z.; Müllen, K. Hexakis(4-iodophenyl)-peri-hexabenzocoronene-A Versatile Building Block for Highly Ordered Discotic Liquid Crystalline Materials. *J. Am. Chem. Soc.* **2004**, *126*, 177–186. [[CrossRef](#)] [[PubMed](#)]
9. Beser, U.; Kastler, M.; Maghsoumi, A.; Wagner, M.; Castiglioni, C.; Tommasini, M.; Narita, A.; Feng, X.; Müllen, K. A C216-nanographene molecule with defined cavity as extended coronoid. *J. Am. Chem. Soc.* **2016**, *138*, 4322–4325. [[CrossRef](#)]
10. Xu, K.; Urgel, J.I.; Eimre, K.; Di Giovannantonio, M.; Keerthi, A.; Komber, H.; Wang, S.; Narita, A.; Berger, R.; Ruffieux, P.; et al. On-surface synthesis of a nonplanar porous nanographene. *J. Am. Chem. Soc.* **2019**, *141*, 7726–7730. [[CrossRef](#)]
11. Kato, K.; Takaba, K.; Maki-Yonekura, S.; Mitoma, N.; Nakanishi, Y.; Nishihara, T.; Hatakeyama, T.; Kawada, T.; Hijikata, Y.; Pirillo, J.; et al. Double-helix supramolecular nanofibers assembled from negatively curved nanographenes. *J. Am. Chem. Soc.* **2021**, *143*, 5465–5469. [[CrossRef](#)]
12. Zhu, X.; Liu, Y.; Pu, W.; Liu, F.-Z.; Xue, Z.; Sun, Z.; Yan, K.; Yu, P. On-Surface Synthesis of C144 Hexagonal Coronoid with Zigzag Edges. *ACS Nano* **2022**, *16*, 10600–10607. [[CrossRef](#)] [[PubMed](#)]
13. Sakamoto, K.; Nishina, N.; Enoki, T.; Aihara, J.-I. Aromatic character of nanographene model compounds. *J. Phys. Chem. A* **2014**, *118*, 3014–3025. [[CrossRef](#)]
14. Jorner, K. Revisiting the superaromatic stabilization energy as a local aromaticity index for excited states. *J. Phys. Org. Chem.* **2022**, *36*, e4460. [[CrossRef](#)]
15. Li, D.; Yang, J.; Cheng, L. A unified superatomic-molecule theory for local aromaticity in π -conjugated systems. *Natl. Sci. Rev.* **2022**, *10*, nwac216. [[CrossRef](#)] [[PubMed](#)]
16. Balasubramanian, K. Density functional and graph theory computations of vibrational, electronic, and topological properties of porous nanographenes. *J. Phys. Org. Chem.* **2022**, *36*, e4435. [[CrossRef](#)]
17. Vivas-Reyes, R.; Martínez-Santiago, O.; Marrero-Ponce, Y. Graph derivative indices interpretation from the quantum mechanics perspective. *J. Math. Chem.* **2023**, *61*, 1739–1757. [[CrossRef](#)]
18. Hosoya, H. Aromaticity index can predict and explain the stability of polycyclic conjugated hydrocarbons. *Monatshfte Fuer Chem./Chem. Mon.* **2005**, *136*, 1037–1054. [[CrossRef](#)]
19. Hosoya, H. Clar's aromatic sextet and sextet polynomial. In *Advances in the Theory of Benzenoid Hydrocarbons*; Springer: Berlin/Heidelberg, Germany, 2005; pp. 255–272.
20. Hosoya, H. Cross-conjugation at the heart of understanding the electronic theory of organic chemistry. *Curr. Org. Chem.* **2015**, *19*, 293–310. [[CrossRef](#)]
21. Hosoya, H. Matching and Symmetry of Graphs. *Comp. Maths. Appl.* **1986**, *12*, 271–290. [[CrossRef](#)]
22. Hosoya, H.; Hosoi, K.; Gutman, I. A Topological Index for the total π -electron Energy. *Theor. Chim. Acta* **1975**, *38*, 37–47. [[CrossRef](#)]
23. Aihara, J.-I.; Yamabe, T.; Hosoya, H. Aromatic character of graphite and carbon nanotubes. *Synth. Met.* **1994**, *64*, 309–313. [[CrossRef](#)]
24. Hosoya, H. Genealogy of Conjugated Acyclic Polyenes. *Molecules* **2017**, *22*, 896. [[CrossRef](#)]
25. Aihara, J.-I. Graph Theory of Ring-Current Diamagnetism. *Bull. Chem. Soc. Jpn.* **2017**, *91*, 274–303. [[CrossRef](#)]
26. Aihara, J.-I. Graph Theory of Aromatic Stabilization. *Bull. Chem. Soc. Jpn.* **2016**, *89*, 1425–1454. [[CrossRef](#)]
27. Balaban, A.T.; Oniciu, D.C.; Katritzky, A.R. Aromaticity as a cornerstone of heterocyclic chemistry. *Chem. Rev.* **2004**, *104*, 2777–2812. [[CrossRef](#)] [[PubMed](#)]
28. Randić, M.; Balaban, A.T. Local aromaticity and aromatic sextet theory beyond Clar. *Int. J. Quantum Chem.* **2018**, *118*, e25657. [[CrossRef](#)]
29. Aihara, J.-I.; Horikawa, T. Graph-Theoretical Formula for Ring Currents Induced in a Polycyclic Conjugated System. *Bull. Chem. Soc. Jpn.* **1983**, *56*, 1853–1854. [[CrossRef](#)]
30. Aihara, J. Magnetotropism of biphenylene and related hydrocarbons. A circuit current analysis. *J. Am. Chem. Soc.* **1985**, *107*, 298–302. [[CrossRef](#)]
31. Aihara, J.-I. Circuit Resonance Energy: A Key Quantity That Links Energetic and Magnetic Criteria of Aromaticity. *J. Am. Chem. Soc.* **2006**, *128*, 2873–2879. [[CrossRef](#)]
32. Aihara, J.-I.; Kanno, H.; Ishida, T. Magnetic resonance energies of heterocyclic conjugated molecules. *J. Phys. Chem. A* **2007**, *111*, 8873–8876. [[CrossRef](#)] [[PubMed](#)]
33. Aihara, J. Topological resonance energy, bond resonance energy, and circuit resonance energy. *J. Phys. Org. Chem.* **2007**, *21*, 79–85. [[CrossRef](#)]
34. Dias, J.R. Valence-Bond Determination of Diradical Character of Polycyclic Aromatic Hydrocarbons: From Acenes to Rectangular Benzenoids. *J. Phys. Chem. A* **2013**, *117*, 4716–4725. [[CrossRef](#)] [[PubMed](#)]

35. Aihara, J.-I.; Makino, M.; Ishida, T.; Dias, J.R. Analytical study of superaromaticity in cycloarenes and related coronoid hydrocarbons. *J. Phys. Chem. A* **2013**, *117*, 4688–4697. [[CrossRef](#)]
36. Dias, J.R. Search for singlet-triplet bistability or biradicaloid properties in polycyclic conjugated hydrocarbons: A valence-bond analysis. *Mol. Phys.* **2012**, *111*, 735–751. [[CrossRef](#)]
37. Dias, J.R. What Do We Know about C₂₄H₁₄ Benzenoid, Fluoranthenoid, and Indacenoid Compounds? *Polycycl. Aromat. Compd.* **2014**, *34*, 177–190. [[CrossRef](#)]
38. Dias, J.R. Nonplanarity Index for Fused Benzenoid Hydrocarbons. *Polycycl. Aromat. Compd.* **2014**, *34*, 161–176. [[CrossRef](#)]
39. Dias, J.R. Perimeter topology of benzenoid polycyclic hydrocarbons. *J. Chem. Inf. Model.* **2005**, *45*, 562–571. [[CrossRef](#)] [[PubMed](#)]
40. Aihara, J.-I. On the Number of Aromatic Sextets in a Benzenoid Hydrocarbon. *Bull. Chem. Soc. Jpn.* **1976**, *49*, 1429–1430. [[CrossRef](#)]
41. Balaban, A.T. To be or not to be Aromatic. *Rec. Roum. Chimie* **2015**, *60*, 121–140.
42. Randić, M. On the role of Kekulé valence structures. *Pure Appl. Chem.* **1983**, *55*, 347–354. [[CrossRef](#)]
43. Randić, M. Aromaticity and Conjugation. *J. Am. Chem. Soc.* **1977**, *99*, 444–450. [[CrossRef](#)]
44. Randić, M. Aromaticity of Polycyclic Conjugated Hydrocarbons. *Chem. Rev.* **2003**, *103*, 3449–3606. [[CrossRef](#)] [[PubMed](#)]
45. Vogler, H. Structures and ¹H-chemical shifts of conjugation deficient hydrocarbons. *Int. J. Quantum Chem.* **1986**, *30*, 97. [[CrossRef](#)]
46. Aihara, J. Is superaromaticity a fact or an artifact? The Kekulene Problem. *J. Am. Chem. Soc.* **1992**, *114*, 865–868. [[CrossRef](#)]
47. Clar, E. *The Aromatic Sextet*; Wiley: London, UK, 1972.
48. Aihara, J.-I. Aromaticity and superaromaticity in cyclopolyacenes. *J. Chem. Soc. Perkin Trans.* **1994**, *2*, 971–974. [[CrossRef](#)]
49. Aihara, J. Lack of Superaromaticity in Carbon Nanotubes. *J. Phys. Chem.* **1994**, *98*, 9773. [[CrossRef](#)]
50. Aihara, J.-I. Hückel-like rule of superaromaticity for charged paracyclophanes. *Chem. Phys. Lett.* **2003**, *381*, 147–153. [[CrossRef](#)]
51. Aihara, J.-I. A Simple Method for Estimating the Superaromatic Stabilization Energy of a Super-Ring Molecule. *J. Phys. Chem. A* **2008**, *112*, 4382–4385. [[CrossRef](#)]
52. Aihara, J. Macrocyclic Conjugation Pathways in Porphyrins. *J. Phys. Chem. A* **2008**, *112*, 5305. [[CrossRef](#)]
53. Dias, J.R.; Aihara, J.-I. Antiaromatic holes in graphene and related graphite defects. *Mol. Phys.* **2009**, *107*, 71–80. [[CrossRef](#)]
54. Makino, M.; Aihara, J. Macrocyclic aromaticity of porphyrin units in fully conjugated oligoporphyrins. *J. Phys. Chem. A* **2012**, *116*, 8074. [[CrossRef](#)]
55. Aihara, J.-I.; Nakagami, Y.; Sekine, R.; Makino, M. Validity and Limitations of the Bridged Annulene Model for Porphyrins. *J. Phys. Chem. A* **2012**, *116*, 11718–11730. [[CrossRef](#)]
56. Dias, J.R. Structure and Electronic Characteristics of Coronoid Polycyclic Aromatic Hydrocarbons as Potential Models of Graphite Layers with Hole Defects. *J. Phys. Chem. A* **2008**, *112*, 12281–12292. [[CrossRef](#)]
57. Dias, J.R. A formula periodic table for benzenoid hydrocarbons and the aufbau and excised internal structure concepts in benzenoid enumerations. *Z. für Natur. A* **1989**, *44*, 765–772. [[CrossRef](#)]
58. Dias, J.R. Concealed Coronoid Hydrocarbons with Enhanced Antiaromatic Circuit Contributions as Models for Schottky Defects in Graphenes. *Open Ophthalmol. J.* **2011**, *5*, 112–116. [[CrossRef](#)]
59. Cyvin, S.J.; Brunvoll, J.; Cyvin, B.N. Theory of Coronoid Hydrocarbons. In *Lecture Notes in Chemistry*; Springer: Berlin, Germany, 1991.
60. Cyvin, S.J.; Brunvoll, J.; Chen, R.S.; Cyvin, B.N.; Zhang, F.J. Theory of Coronoid Hydrocarbons II. In *Lecture Notes in Chemistry*; Springer: Berlin, Germany, 1994; Volume 62.
61. Gutman, I.; Milun, M.; Trinajstić, N. Graph theory and molecular orbitals. 19. Nonparametric resonance energies of arbitrary conjugated systems. *J. Am. Chem. Soc.* **1977**, *99*, 1692. [[CrossRef](#)]
62. Aihara, J.-I.; Kanno, H. Local Aromaticities in Large Polyacene Molecules. *J. Phys. Chem. A* **2005**, *109*, 3717–3721. [[CrossRef](#)]
63. Sekine, R.; Nakagami, Y.; Aihara, J. Aromatic Character of Polycyclic π Systems Formed by Fusion of Two or More Rings of the Same Size. *J. Phys. Chem. A* **2011**, *115*, 6724. [[CrossRef](#)] [[PubMed](#)]
64. Saito, S.; Osuka, A. Expanded Porphyrins: Intriguing Structures, Electronic Properties, and Reactivities. *Angew. Chem. Int. Ed.* **2011**, *50*, 4342–4373. [[CrossRef](#)]
65. Randić, M.; Balaban, A.T.; Plavšić, D. Applying the conjugated circuits method to Clar structures of [n]phenylenes for determining resonance energies. *Phys. Chem. Chem. Phys.* **2011**, *13*, 20644–20648. [[CrossRef](#)] [[PubMed](#)]
66. Balasubramanian, K.; Kaufman, J.J.; Koski, W.S.; Balaban, A.T. Graph theoretical characterization and computer generation of certain carcinogenic benzenoid hydrocarbons and identification of bay regions. *J. Comput. Chem.* **1980**, *1*, 149–157. [[CrossRef](#)]
67. Balasubramanian, K. Graph-Theoretical Characterization of Fullerene Cages. *Polycycl. Aromat. Compd.* **1993**, *3*, 247–259. [[CrossRef](#)]
68. Arockiaraj, M.; Clement, J.; Balasubramanian, K. Topological Indices and Their Applications to Circumcised Donut Benzenoid Systems, Kekulenes and Drugs. *Polycycl. Aromat. Compd.* **2018**, *40*, 280–303. [[CrossRef](#)]
69. Arockiaraj, M.; Paul, D.; Clement, J.; Tigga, S.; Jacob, K.; Balasubramanian, K. Novel molecular hybrid geometric-harmonic-Zagreb degree based descriptors and their efficacy in QSPR studies of polycyclic aromatic hydrocarbons. *SAR QSAR Environ. Res.* **2023**, *34*, 569–589. [[CrossRef](#)] [[PubMed](#)]
70. Balasubramanian, K. Applications of Combinatorics and Graph Theory to Quantum Chemistry & Spectroscopy. *Chem. Rev.* **1985**, *85*, 599–618.
71. Ramaraj, R.; Balasubramanian, K. Computer Generation of Matching Polynomials of Graphs and Lattices. *J. Comput. Chem.* **1985**, *6*, 122–141. [[CrossRef](#)]

72. Balasubramanian, K.; Randić, M. Characteristic Polynomials of Structures with Pending Bonds. *Theor. Chim. Acta* **1982**, *61*, 307–323. [[CrossRef](#)]
73. Balasubramanian, K. Characteristic polynomials of organic polymers and periodic structures. *J. Comput. Chem.* **1985**, *6*, 656–661. [[CrossRef](#)]
74. Balasubramanian, K. Spectra of matching polynomials. *Chem. Phys. Lett.* **1993**, *208*, 219–224. [[CrossRef](#)]
75. Manoharan, M.; Balakrishnarajan, M.; Venuvanalingam, P.; Balasubramanian, K. Topological resonance energy predictions of the stability of fullerene Clusters. *Chem. Phys. Lett.* **1994**, *222*, 95–100. [[CrossRef](#)]
76. Balasubramanian, K. Matching Polynomials of Fullerene Clusters. *Chem. Phys. Lett.* **1993**, *201*, 306–314. [[CrossRef](#)]
77. Balasubramanian, K. Symmetry and Combinatorial Concepts for Cyclopolymers, Nanotubes and 2D-Sheets: Enumerations, Isomers, Structures Spectra & Properties. *Symmetry* **2021**, *14*, 34. [[CrossRef](#)]
78. Hosoya, H.; Balasubramanian, K. Computational Algorithms for Matching Polynomials of Graphs from the Characteristic Polynomials of Edge-Weighted Graphs. *J. Comput. Chem.* **1989**, *10*, 698–710. [[CrossRef](#)]
79. Hosoya, H.; Balasubramanian, K. Exact Dimer Statistics and Characteristic-Polynomials of Cacti Lattices. *Theor. Chim. Acta* **1989**, *76*, 315–329. [[CrossRef](#)]
80. Balasubramanian, K. Symmetry, Combinatorics, Artificial Intelligence, Music and Spectroscopy. *Symmetry* **2021**, *13*, 1850. [[CrossRef](#)]
81. Herndon, W.C. Resonance energies of aromatic hydrocarbons. Quantitative test of resonance theory. *J. Am. Chem. Soc.* **1973**, *95*, 2404–2406. [[CrossRef](#)]
82. Moreno-Vicente, A.; Abella, L.; Azmani, K.; Rodriguez-Fortea, A.; Poblet, J.M. Formation of C_{2v}-C₇₂ (11188)C₁₄: A Particularly Stable Non-IPR Fullerene. *J. Phys. Chem. A* **2018**, *122*, 2288–2296. [[CrossRef](#)] [[PubMed](#)]
83. Chen, Z.; Cioslowski, J.; Rao, N.; Moncrieff, D.; Bühl, M.; Hirsch, A.; Thiel, W. Endohedral chemical shifts in higher fullerenes with 72–86 carbon atoms. *Theor. Chem. Accounts* **2001**, *106*, 364–368. [[CrossRef](#)]
84. Ishfaq, F.; Nadeem, M.F.; El-Bahy, Z.M. On topological indices and entropies of diamond structure. *Int. J. Quantum Chem.* **2023**, *123*, e27207. [[CrossRef](#)]
85. Al-Dayel, I.; Nadeem, M.F.; Khan, M.A. Topological analysis of tetracyanobenzene metal–organic framework. *Sci. Rep.* **2024**, *14*, 1789. [[CrossRef](#)] [[PubMed](#)]

Disclaimer/Publisher’s Note: The statements, opinions and data contained in all publications are solely those of the individual author(s) and contributor(s) and not of MDPI and/or the editor(s). MDPI and/or the editor(s) disclaim responsibility for any injury to people or property resulting from any ideas, methods, instructions or products referred to in the content.